PHYSICAL REVIEW E **79**, 010601(R) (2009)

Ripening-dominated crystallization in polydisperse hard-sphere-like colloids

Sara Iacopini, Thomas Palberg, and Hans Joachim Schöpe
Institut für Physik, Johannes Gutenberg Universität Mainz, Staudingerweg 7, D-55128 Mainz, Germany
(Received 14 July 2008; revised manuscript received 6 November 2008; published 28 January 2009)

We report on the crystal growth scenario in gravity-matched, polydisperse hard-sphere-like colloids at increasing particle concentration. In the fluid-crystal coexistence region, the crystal size as a function of time shows two separate regimes corresponding to crystal growth and crystal ripening. At higher supersaturation the crystal size grows according to the same power law through the whole experimental window of a few days: crystal growth and ripening merge together. We show that our observations cannot be explained by considering the slowing down of single-particle dynamics due to increasing volume fraction. We suggest that size fractionation occurring at the crystal-fluid interface is the dominant mechanism.

DOI: 10.1103/PhysRevE.79.010601 PACS number(s): 64.75.Gh, 81.10.Fq, 82.70.Dd

In the classical crystallization scenario, three processes can be discriminated: crystal nucleation, growth, and ripening. The crystallization kinetics and the resulting morphology of the polycrystalline material are given by a complex interplay of these mechanisms. In the case of "polydisperse" systems, where polydispersity indicates any heterogeneity in the properties of the components, the scenario is further complicated by partitioning of different species between the coexisting phases [1].

Colloidal hard spheres, which form a crystal phase when the suspension is supersaturated above a particle volume fraction of about 50% [2,3], provide an extremely convenient model system for investigating solidification kinetics [4] with easily accessible experimental techniques such as laser light scattering [5–9] and microscopy [10], allowing also access to the very early stage of solidification [11–13]. Seminal works performed by van Megen and co-workers have investigated the influence of the sample supersaturation [14] and of the sample size polydispersity [6] on the crystallization kinetics. Later the role of size heterogeneity and the influence of fractionation [9,12,13] were studied, finally evidencing that crystal nucleation in polydisperse hard spheres is a two-step process [12]. According to the resulting scenario, the appearance of crystals is preceded by the formation of crystal precursors, densely packed domains with at most only partial crystalline order, which have to be converted into proper crystals before they can grow. The time needed for the precursor conversion as well as for the crystallization process increases strongly with polydispersity [6,13], thus supporting the hypothesis that fluid-to-crystal conversion involves particle size fractionation.

While the works mentioned above have collected and interpreted important evidence concerning the appearance of the crystal phase inside the metastable melt, to our knowledge no one has ever analyzed in detail the growth of converted precursors, depending on the sample supersaturation. Harland and van Megen have already qualitatively shown how crystallization kinetics changes upon increasing the sample volume fraction [14], clarifying that at high supersaturations growth is suppressed due to competition with high nucleation rates [5]. An explanation of the systematic changes in the growth behavior observed upon increasing the volume fraction in terms of existing models is still missing. The literature refers occasionally to the classical laws of interface-limited ($L \sim t$) and diffusion-limited ($L \sim t^{1/2}$) growth of the crystal size L, without commenting on the extension of their validity in describing experimental data.

In this paper we focus on the analysis of crystal growth in polydisperse hard spheres in the concentration range where the crystal growth kinetics changes from being diffusion limited to being suppressed by accelerated nucleation [5]. This transition is characterized by the emerging of a "ripening-dominated" regime, where the distinction between early stage (precursors' conversion and growth) and late stage (ripening) in terms of the crystal growth law is completely canceled. These observations are compared with an existing model for growth, and the relevance of size fractionation effects is pointed out and discussed.

We used 1:10 cross-linked hard-sphere-like polystyrene (PS) microgel colloids [15] dispersed in the good solvent 2-ethyl-naphthalene (2EN), which has the same refractive index of PS and very similar density ($n_{PS}=1.598$, $n_{2EN}=1.599$, $d_{PS}=1.05$ g cm^{-3}, $d_{2EN}=0.992$ g cm^{-3}). These samples provide hard-sphere-like systems with negligible gravity effects. The particle size $R=(423\pm3)$ nm and polydispersity $\sigma\approx6.5\%$ were estimated using established light-scattering methods [16]. The polydispersity of our samples exceeds the limiting value of $\sim5.7\%$ that can be hosted by a single crystal [2]; size fractionation of some extent during solidification is therefore necessary. The concentration scale was set by locating the observed freezing point at the volume fraction value expected for hard spheres with $\sigma=6.5\%$: $\Phi_{fr}=0.515$ [2]. The melting point, obtained by extrapolating the crystal fraction observed in coexistence to 100%, is then at $\Phi_m=(0.554\pm0.002)$. The crystallization kinetics was monitored by time-resolved Bragg light scattering, using an apparatus that allows for averaging the scattered intensity over the whole Debye-Scherrer cone. Compared to previously employed analogous instruments [17], our spectrometer covers a much broader q range ($4\leqslant q\leqslant19$ μm^{-1}), including the main and higher-order Bragg reflections from the crystals [Fig. 1(a)], with a nominal resolution of about 0.002 μm^{-1}. The setup will be described in more detail in a future publication [18]. The samples were shear-molten prior to measuring by tumbling for several hours at a frequency of ≈1 Hz. The first light-scattering acquisition ends typically 90 s after cessation of shear melting: we set this as the time $t=0$ when, we assume, the system is still in the metastable fluid state.

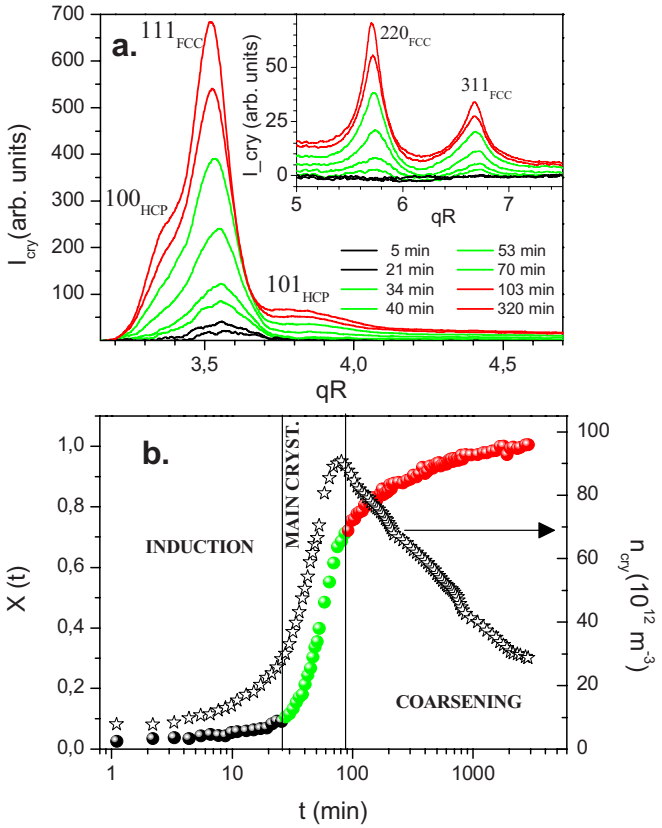

FIG. 1. (Color online) Basic crystallization kinetics features for sample $M2$ ($\Phi=0.557$). (a) Evolution of the crystal scattering intensity at the main reflections and (inset) at the higher-order reflections. (b) Time evolution of the crystallinity $X(t)$ (spheres, left axis) and the number density of crystallites (stars, right axis). The color code in the crystallinity curve and in the scattering curves in (a) corresponds to the different crystallization stages: black $\equiv$induction, green (lighter gray) $\equiv$main crystallization, red (gray) $\equiv$coarsening (ripening).

The subsequent emerging of the crystal phase is monitored with a time resolution of up to 60 s and characterized by the scattering intensity from the crystal: $I_{\mathrm{cry}}(q,t)=I(q,t)-\beta(t)I(q,0)$, where I denotes the measured intensity and $\beta(t)$ is a scaling factor accounting for the decreasing scattering from the fluid [5]. The time evolution of single Bragg peaks is analyzed by performing a best fit with a Gauss function. As we are analyzing scattered intensities instead of absolute structure factors, only Bragg peaks located at a sufficient distance from the form-factor minimum can be analyzed, giving the identical information as a structure factor analysis. From the fit parameters $A(t)$ (integrated area of the peak) and $w(t)$ (full width at half maximum of the peak), the following information can be obtained: (i) the crystallinity $X(t)$ (the fraction of the sample which is crystalline): $X(t)=cA(t)$, where c is a normalization factor based on the equilibrium phase diagram; (ii) the average linear dimension of the crystallites $L(t)$: $L(t)=2\pi K/w(t)$, where K is the Scherrer constant ($K=1.107$ for crystallites of spherical shape); (iii) the number density of crystallites: $n_{\mathrm{cry}}(t)=X(t)/\langle L^3(t)\rangle=X(t)/\alpha[L(t)]^3$, where the parameter $\alpha\approx 1.25$ relates the average crystal size cubed, with the average crystal volume [13].

We have considered concentrations ranging from $\Phi=0.551$ ($M1$) to $\Phi=0.568$ ($M5$)—i.e., from slightly below the melting point to deep in the fully crystalline region. The reproducibility of the results was checked by repeating the measurements on a new set of samples. Figure 1 illustrates general features of polydisperse hard-sphere crystallization kinetics. Figure 1(a) shows the evolution of I_{cry}, displaying the Bragg reflections typical of a random hexagonal close-packed (RHCP) structure [7]. Crystallization always starts with the appearance of a broad, slowly growing, single peak around the main Bragg reflection, signaling the nucleation of crystal precursors [12]. Their conversion into true RHCP crystals is signaled by the first appearance of the higher-order reflections: this happens at the induction time t_{ind}. Thereafter the phase transition proceeds faster: converted precursors grow and new crystals appear, while the crystallinity X grows from about 10% (typical value at t_{ind}) to close to 100% [Fig. 1(b)]. This stage is denoted the main crystallization. The following stage is identified with ripening of the polycrystal: the number of crystallites decreases, while their average dimension increases. It begins at the time t_{coars} when the number of crystals starts to drop [Fig. 1(b)].

The growth kinetics of the average crystal dimension L depending on supersaturation is shown in Fig. 2(a). In agreement with previous investigations, we observe precursors with always approximately the same dimensions during induction [13] and we see that at high supersaturation ($M5$) crystallization is dominated by nucleation and crystal size increase takes place only in the late stage ($t\gtrsim t_{coars}$), due to ripening [5]. The growth of crystals during the main crystallization, which is significant in coexistence ($M1$), shrinks gradually as supersaturation is increased ($M2$,$M3$,$M4$). Samples with volume fractions in the range delimited by $M3$ ($\Phi=0.559$) and $M4$ ($\Phi=0.565$) show a peculiar and so far not noticed behavior. The distinction between two different growth regimes before and after t_{coars} is lost. The growth of crystallites can be very well described by a single power law from t_{ind} up to the longest considered times [Fig. 2(b)].

The "classical" growth of hard-sphere colloidal crystals has been described by Ackerson and Schätzel [19]. This approach assumes the growth of crystallites by addition of individual particles from the melt, and the velocity of the crystal boundary is estimated through the Wilson-Frenkel law: $dx/d\tau=\delta[1-\exp(\Delta\mu/K_BT+cx)]$, where $x=L/l$ and $\tau=D_0t/l^2$ are the reduced linear crystal dimension and reduced time, respectively, l is the dimension of the critical nucleus, D_0 is the free-particle diffusion coefficient, $\Delta\mu$ is the chemical potential difference between the solid and fluid phases, c is a surface energy constant giving zero growth velocity for a critical nucleus, and δ is a kinetic coefficient proportional to the self-diffusion constant $D_S(\Phi)$ that governs the attachment of particles to the crystal (Φ denotes the volume fraction of the melt). Fractionation effects, such as selective inclusion of particles of the proper size into the crystal, are not explicitly taken into account. Growth results are given in terms of an instantaneous growth exponent $\eta(\tau)$: $x(\tau)\sim\tau^{\eta(\tau)}$ (Fig. 7 of Ref. [19]). The growth exponent $\eta(\tau)$ approaches the "classical" constant values of 0.5 or 1 after staying on much lower values ($\sim$0.1) for time intervals that can become very long as δ decreases. In order to attempt a comparison between the

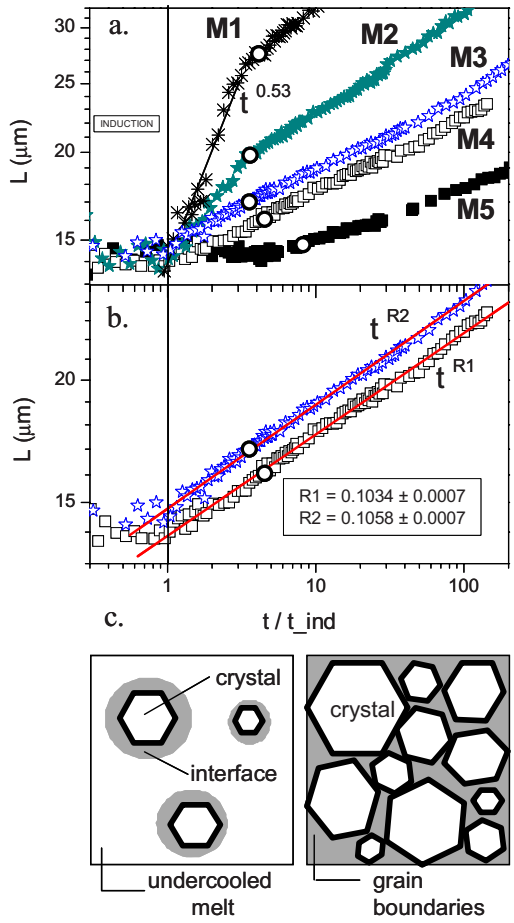

FIG. 2. (Color online) (a) Time evolution of the crystallites' dimensions: asterisks ($M1$, $\Phi=0.551$), solid stars ($M2$, $\Phi=0.557$), open stars ($M3$, $\Phi=0.559$), open squares ($M4$, $\Phi=0.565$), and solid squares ($M5$, $\Phi=0.568$). The time scale for each sample is normalized on t_{ind}, which is (25 ± 5) min for all samples considered here. Circles denote the position of t_{coars} for each sample. The solid line is a best fit with a power law for sample $M1$ during main crystallization. (b) Samples $M3$ and $M4$, displaying "ripening-dominated" growth from the very beginning of crystallization. Solid lines are power-law best fits to the data, starting from $t/t_{ind}=1$. (c) Schematic illustrating the hypothetic structure of a polydisperse crystallizing sample during the early stage of the main crystallization (left) and during ripening (right). According to our hypothesis, particle transport in the gray regions governs crystal growth in both cases.

theory and our experiment, we considered that $\tau=0$ corresponds to t_{ind}—i.e., to the first appearance of converted precursors, whose dimension l is ~ 14 μm; the characteristic time l^2/D_0 for our colloids is about 20 min. Sample $M1$ reaches the asymptotic behavior $L\sim t^{1/2}$ less than 10 min after t_{ind} ($\tau\approx 0.5$). By comparison with Fig. 7 of Ref. [19], it behaves like a system with at least $\delta=10$. Sample $M3$ maintains 60 min after t_{ind} ($\tau\approx 3$) an instantaneous growth exponent close to 0.1: this is compatible with the behavior of systems with δ as low as 0.01; i.e., we observe a decrease of the kinetic coefficient of at least three orders of magnitude upon an increase from 0.551 to 0.559 in the volume fraction. This occurs as the volume fraction is still far from the value of 0.58, where the glass transition is expected [3]. In the model, δ depends on the diffusion constant governing the movement of the crystal boundary; assuming that this corresponds to the single-particle long-time diffusion coefficient and by adopting the empirical expression used by Harland and van Megen [14], we calculate, upon the given volume fraction increase, a kinetic coefficient decrease of only about a factor of 2. The observed slowing down of crystallization cannot be explained in terms of the slowing down of single-particle dynamics due to the increase of packing. We think that fractionation effects have in this a critical role.

The coarsening times normalized with the induction times show a weak dependence on particle concentration: the start of the main crystallization process and the start of coarsening are closely related. During the main crystallization, samples $M3$ and $M4$ are trapped into a transient process that merges with ripening: asymptotic growth is not reached. All this suggests that similar particle transport mechanisms govern the growth in both stages: when the crystals grow in the supersaturated melt and when, in the late stage, the sample is crowded with crystals that exchange particles through the grain boundaries. A possible crystallization scenario where this occurs is depicted in Fig. 2(c). The growing crystal is surrounded by an extended interface region, with density and structure intermediate between those of the crystal and the melt. Dullens and co-workers [20] have measured the thickness of the fluid-crystal interface for sedimenting colloids using confocal microscopy. Out of equilibrium (i.e., when the fluid on top of the crystal is undercooled), the interface thickness extends up to 15 particle diameters. We assume that inside this interface slow-particle rearrangements, limited by high density and partial caging, govern the attachment of colloids of the proper size to the crystal boundary. Similarly, the exchange of particles between ripening crystals in the late stage occurs through particle fractionation inside partially crystalline, partially amorphous grain boundaries. In the frame of this scenario, the kinetic coefficient governing the growth of crystals depends in both cases on the efficiency of size fractionation inside a dense, partially crystalline environment and cannot be expressed only in terms of single particle dynamics.

The existence of an extended interface fits into a two-step nucleation scenario, already suggested by different authors [1,12,21]: the metastable polydisperse fluid relaxes the density first by producing distorted crystalline structures with a quenched size distribution; later, the optimal particle fractionation and crystal structure is achieved.

To conclude, we have examined the crystal growth kinetics at increasing supersaturation for hard-sphere-like colloids with size polydispersity high enough, such that fractionation effects cannot be avoided. We have shown that the observed slowing down of crystallization cannot be explained in terms of the slowing down of single-particle dynamics. On the basis of the observation of long-living growth transients that merge with the ripening process, we suggested that crystal growth is governed by particle fractionation inside an extended interface region surrounding the growing crystallite. The existence of such an interface region supports a two-step nucleation scenario where, due to sample polydispersity and consequent requirement of species partitioning, the system relaxes the density first and only on longer time scales tries to achieve the optimal structure.

We thank E. Bartsch for the kind gift of the particles. The financial support of Grant No. DFG SFB-TR6, the Forschungsfond der Universität Mainz, and Grant No. DFG SPP 1296 is gratefully acknowledged. S.I. acknowledges funding from the Marie Curie Research and Training Network MRTN-CT-2003-504712.

[1] P. Bartlett, J. Phys.: Condens. Matter **12**, A275 (2000); R. M. L. Evans and C. B. Holmes, Phys. Rev. E **64**, 011404 (2001); P. B. Warren, Phys. Chem. Chem. Phys. **1**, 2197 (1999); M. Fasolo and P. Sollich, Phys. Rev. E **70**, 041410 (2004).
[2] P. G. Bolhuis and D. A. Kofke, Phys. Rev. E **54**, 634 (1996).
[3] P. N. Pusey and W. van Megen, Nature (London) **320**, 340 (1986).
[4] V. J. Anderson and H. N. W. Lekkerkerker, Nature (London) **416**, 811 (2002).
[5] J. L. Harland, S. I. Henderson, S. M. Underwood, and W. van Megen, Phys. Rev. Lett. **75**, 3572 (1995).
[6] S. I. Henderson and W. van Megen, Phys. Rev. Lett. **80**, 877 (1998).
[7] P. N. Pusey *et al.*, Phys. Rev. Lett. **63**, 2753 (1989).
[8] K. Schätzel and B. J. Ackerson, Phys. Rev. Lett. **68**, 337 (1992).
[9] S. Martin, G. Bryant, and W. van Megen, Phys. Rev. E **67**, 061405 (2003); **71**, 021404 (2005).
[10] D. J. W. Aastuen, N. A. Clark, L. K. Cotter, and B. J. Ackerson, Phys. Rev. Lett. **57**, 1733 (1986); P. Wette *et al.*, J. Chem. Phys. **123**, 174902 (2005).
[11] U. Gasser *et al.*, Science **292**, 258 (2001).
[12] H. J. Schöpe, G. Bryant, and W. van Megen, Phys. Rev. Lett. **96**, 175701 (2006).
[13] H. J. Schöpe *et al.*, J. Chem. Phys. **127**, 084505 (2007).
[14] J. L. Harland and W. van Megen, Phys. Rev. E **55**, 3054 (1997).
[15] E. Bartsch *et al.*, Ber. Bunsenges. Phys. Chem. **102**, 1597 (1998).
[16] H. J. Schöpe *et al.*, Langmuir **23**, 11534 (2007).
[17] P. S. Francis *et al.*, Rev. Sci. Instrum. **73**, 3878 (2002).
[18] S. Iacopini, T. Palberg, and H. J. Schöpe, J. Chem. Phys. (to be published).
[19] B. J. Ackerson and K. Schätzel, Phys. Rev. E **52**, 6448 (1995).
[20] R. P. A. Dullens, D. G. A. L. Aarts, and W. K. Kegel, Phys. Rev. Lett. **97**, 228301 (2006).
[21] J. F. Lutsko and G. Nicolis, Phys. Rev. Lett. **96**, 046102 (2006); P. G. Vekilov, Cryst. Growth Des. **4**, 671 (2004).